Phys Chem Minerals (2003) 30: 271–279
DOI 10.1007/s00269-003-0314-6

ORIGINAL PAPER

E. Thurel · J. Douin · P. Cordier

Plastic deformation of wadsleyite: III. Interpretation of dislocations and slip systems

Received: 15 July 2002 / Accepted: 14 February 2003

Abstract Linear anisotropic elasticity has been applied to interpret the dislocation stability and ease of slip in wadsleyite. It is shown that wadsleyite is very isotropic from the elastic point of view. The influence of crystal chemistry and bonding on the choice of the slip plane is discussed. It is shown that slip is predominantly achieved on planes that do not shear Si–O bonds. It is suggested that dissociation of dislocations is essential in determining the ease of slip among the various slip systems.

Keywords Linear anisotropic elasticity · Dislocation stability · Slip planes

Introduction

It is now possible to investigate the physical properties of minerals at pressures and temperatures of the deep Earth. In particular, and despite serious present-day limitations, we are now able to induce plastic deformation in minerals at P, T conditions relevant for the Earth's transition zone. Parts I and II of the present study describe plastic deformation experiments in shear and compression geometry performed on wadsleyite. Subsequent investigation of the dislocation microstructures by transmission electron microscopy (TEM) using large-angle convergent beam microscopy (LACBED) has yielded much information on the various dislocations which can glide in the wadsleyite structure, on their slip planes, on their possible dissociations, etc. Several slip systems have been identified:

$[100](010)$
$[100](001)$
$[100]\{011\}$
$[100]\{021\}$
$1/2\langle 111\rangle\{101\}$
$[010](001)$
$[010]\{101\}$
$\langle 101\rangle(010)$,

although only those involving $1/2\langle 111\rangle$ and [100] dislocation appear to be easily activated at high temperature (Part II).

In the present study, we first examine the elastic properties of wadsleyite. Then, we examine the influence of crystal chemistry on the choice of the slip plane. Finally, anisotropic elasticity is applied to calculate the non-core, elastic energy of dislocations in wadsleyite. The possible influence of dissociation on the choice of the slip systems is also discussed.

Elasticity

Before considering the plastic behaviour, it might be interesting to discuss the elastic properties of wadsleyite. Seismic data being one of the richest sources of information on the structure of the mantle, it early appeared important to determine the elastic properties of mantle minerals at both high P and high T. Important work has been accomplished in this direction in recent years from the experimental side (Liebermann and Li 1998; Liebermann 2000) as well as from the theoretical side (Sixtrude 2000). Several studies have established the evolution of the shear modulus and bulk modulus of wadsleyite with pressure (Sawamoto et al. 1984; Gwamnesia et al. 1990;

E. Thurel · P. Cordier (✉)
Laboratoire de Structure et Propriétés de l'Etat Solide,
UMR CNRS 8008, Université des Sciences et
Technologies de Lille, France
e-mail: Patrick.Cordier@univ-lille1.fr
Tel.: +33 320 43 43 41
Fax: +33 320 43 65 91

J. Douin
Laboratoire d'Etude des Microstructures,
UMR 104 CNRS/ONERA, France

P. Cordier
Bayerisches Geoinstitut,
Universität Bayreuth, Germany

Table 1 Elastic moduli of wadsleyite as a function of pressure from Zha et al. (1998)

P (GPa)	C_{11} (GPa)	C_{22} (GPa)	C_{33} (GPa)	C_{44} (GPa)	C_{55} (GPa)	C_{66} (GPa)	C_{12} (GPa)	C_{13} (GPa)	C_{23} (GPa)
0	370.5	367.5	272.5	111	122	103	65	95	105
3.1	379	382	292	111	122.5	100.5	85.5	105.5	112.5
6.3	393.5	400	317	126.5	117.5	117	84	118	119
8.1	404	418.5	324	121.5	123.5	118.5	94.5	122.5	123.5
9.4	414.5	440	333	127	123	118.5	104	124	132
10.1	429	416	334	117.5	128	121	104.5	130	111
10.5	422	425.5	331	121.5	127	116	108	128	125.5
14.2	444.5	465	387	131	121.5	130	124	142	152

Li et al. 1996; Li et al. 1998, Sinogeikin et al. 1998; Zha et al. 1998; Li and Liebermann 2000). The influence of temperature at pressures up to 7 GPa has been addressed recently by Li et al. (1998). Measurements performed on single crystals allow determination of the nine independent coefficient of the matrix which, in Voigt notation, describe the fourth-rank tensor of elastic constants (Sawamoto et al. 1984; Sinogeikin et al. 1998; Zha et al. 1998). The results of Zha et al. (1998), which extend to ca 14 GPa, have been used in the following of this study. They are presented in Table 1.

In a crystal which is potentially anisotropic, the shear modulus, which describes the resistance of the structure to shear, has to be defined in a given plane and along a given direction. We have used anisotropic elasticity to calculate the shear modulii corresponding to the various slip systems observed in wadsleyite. It is possible for a given shear direction such as [100] to calculate the shear modulus in any plane (0kl) containing the shear direction. The details of the calculation are given in Appendix 1. The evolution of the shear modulus $\mu_{[100](0kl)}$ with the orientation of the shear plane is presented Fig. 1 at two different pressures. The result of a similar calculation for shear along [010] is given Fig. 2. It shows that for a given shear direction, the choice of the glide plane is probably not governed by elasticity, as the elastic properties do not vary much with the orientation of the plane. We have plotted in Fig. 3 the evolution with pressure of the shear modulii corresponding to various slip systems. Except for $\mu_{[100](001)}$, which has a small dependence with pressure, the other shear moduli have a very similar evolution. They increase by about 20% when pressure is raised from room pressure to 14 GPa. The different slip systems face very comparable shear moduli and their differences even decrease with increasing pressure. The choice of the easy slip systems is then unlikely to result from elasticity only, as wadsleyite appears to have a very isotropic behaviour from the elastic point of view.

Slip planes

In metals, the glide planes are usually selected among the close-packed planes. In the case of oxides, one usually looks for close-packing within the oxygen sublattice. This approach has been followed by Dupas et al. (1994), who noted that the oxygen sublattice of wadsleyite is face-centred cubic. Their observation that slip does take place in the {021} and {101} planes (which belong to close-packed planes of the anionic sublattice) was interpreted accordingly. In the case of silicates, one must

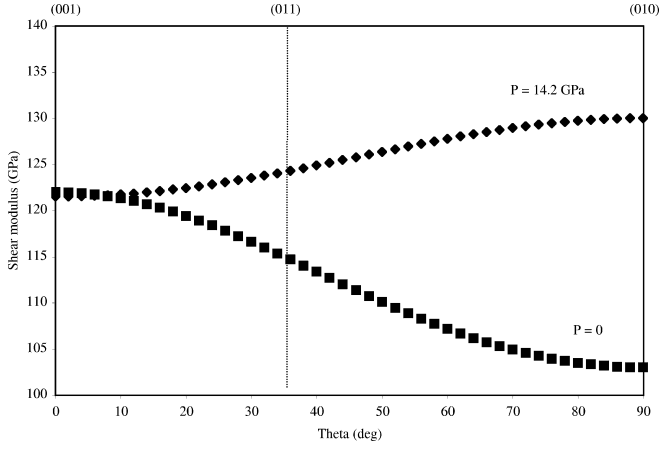

Fig. 1 Shear modulus along [100] in a plane (0kl). Theta is the angle between (0kl) and (001). The shear modulii are calculated at two pressures 0 and 14.2 GPa by using the elastic data of Zha et al. (1998) presented in Table 1

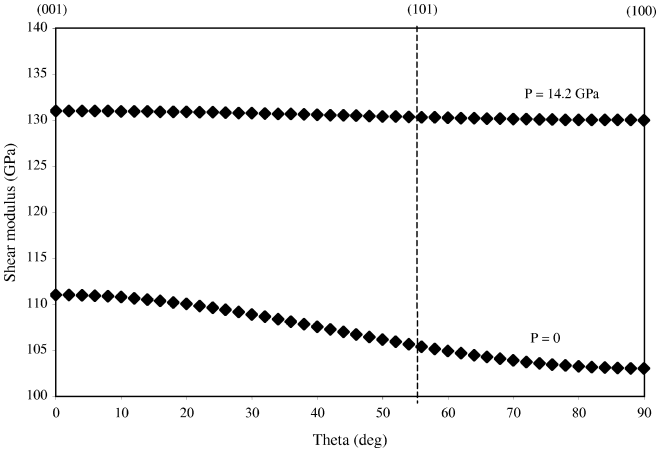

Fig. 2 Shear modulus along [010] in a plane (0kl). Theta is the angle between (h0l) and (001). The shear modulii are calculated at two pressures 0 and 14.2 GPa by using the elastic data of Zha et al. (1998) presented in Table 1

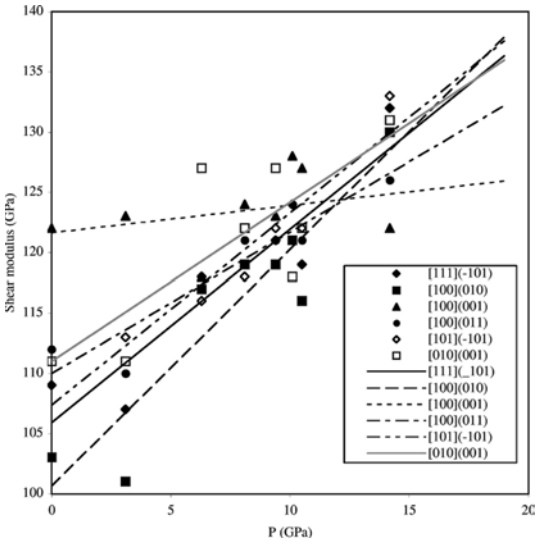

Fig. 3 Evolution with pressure of the shear moduli corresponding to the main slip system characterized in wadsleyite. The elastic data are taken from Zha et al. (1998)

take into account the nature of the bonds that the dislocation has to break in its glide motion. Indeed, wadsleyite is built up with two distinct structural units: MgO_6 octahedra and Si_2O_7 units constituted of two linked SiO_4 tetrahedra. The Si–O bonds, which are the shorter, are the strongest bonds of the structure. Figure 4 presents the unit cell of wadsleyite viewed along [100] and [010]. One can see that (010), (001), {101} and {011}, which have been identified as glide planes in our study, are planes which allow shear without cutting the strong Si–O bonds. It is only in the case of {021} that shear is likely to be accompanied by the breaking of Si–O bonds.

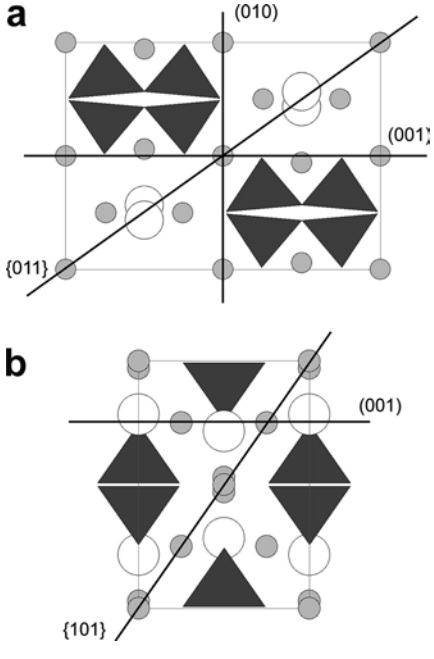

Fig. 4 Unit cell of wadsleyite viewed along [100] (**a**) and [010] (**b**). Only the SiO_4 tetrahedra are represented. The slip planes characterized in wadsleyite are shown

Dislocation and slip systems

In this section, we examine the energetics of dislocations in wadsleyite. The energy of a dislocation is made of two contributions. One is due to the breaking and distortion of the bonds in the dislocation core, and can be determined through atomistic calculations. The second is the elastic energy stored in the crystal. We will consider this latter term only, which can be calculated using anisotropic elasticity. In a crystal, the elastic energy of a straight dislocation per unit length is given by:

$$E = K\frac{b^2}{4\pi}\mathrm{Ln}\left(\frac{R}{r_0}\right)$$

where b is the magnitude of the Burgers vector, R is the radius of the dislocation strain field, r_0 is the dislocation core radius and K is a factor which is a function of the elastic constants of the crystal and of the character of the dislocation line. In this study, the energy term E has been calculated with the help of DISDI, a program based on Stroh's (1958) formalism, using the ANCALC subroutine originally designed by Head et al. (1973) and subsequently modified to include any crystal structure and dissociated dislocations. In every case, R has been taken equal to 100 nm. The actual value of r_0 is unknown. Without these data, we have, for the sake of simplicity, used a constant value of 0.3 nm for every dislocation. An alternative option could have been to use a value of r_0 proportional to the modulus of the Burgers vector. We have checked that this option would not have qualitatively changed the results obtained.

[100] slip

Dislocations with [100] Burgers vector have been observed and characterized in every sample. They are usually straight with a marked screw character. [100] slip represents clearly a major deformation mode. Moreover, the shear experiments suggest that [100] slip is easy at high temperature. The slip system [100]{021} had already been reported by Dupas et al. (1994) while Sharp et al. (1994) observed [100] dislocations gliding in (010) in a San Carlos olivine deformed at 14 GPa and 1450 °C. In our study, [100] dislocations have been found to glide in (001), (010), {011} and {021}. The elastic energy per unit length of [100] dislocations lying in these planes has been calculated with DISDI as a function of the dislocation character. The results are presented in Fig. 5. One can see that, in agreement with the conclusion of the previous section on the weak anisotropic character of wadsleyite, the energy difference is small between the different slip planes. One can see also

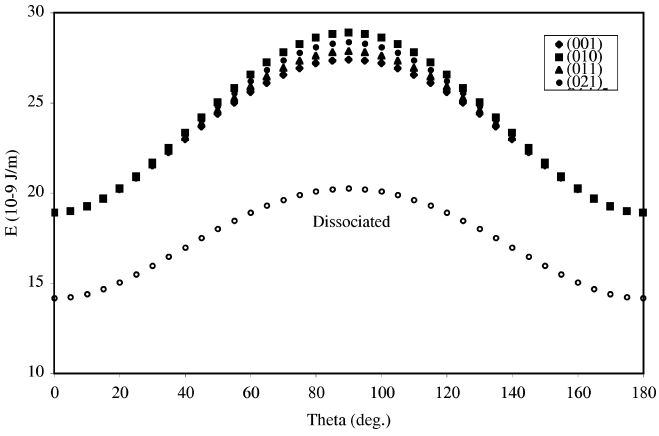

Fig. 5 Elastic energy per unit length of [100] dislocations lying in various planes (*solid symbols*): (001), (010), (011) and (021) (calculated with DISDI). Theta is the angle between the dislocation line and the Burgers vector. It represents the dislocation character (theta = 90° for the edge dislocation and theta = 0° or 180° for the screw dislocation). The *open circles* represent the elastic energy per unit length of [100] dislocations dissociated in (021) into two 1/2[100] partial dislocations separated by a stacking fault with an energy of 110 mJ m^{-2}

that the elastic energy of a dislocation is significantly lower for screw ($\theta = 0$ or 180°) than for edge orientation ($\theta = 90°$), as expected in an almost isotropic material for which the ratio (elastic $\text{energy}_{\text{edge}}$)/(elastic $\text{energy}_{\text{screw}}$) is close to 1.5. However, this difference alone is unlikely to account for the marked screw character observed experimentally, which probably reflects some favourable core structure. In one case only have we observed dissociated [100] dislocations. These were dissociated in their glide plane: {021} and the partial separation was of the order of 15 nm. Although the Burgers vector of the partial dislocations has not been fully characterized, the contrast observed suggests the simple reaction: [100] → 1/2[100] + 1/2[100]. This scenario is also supported by the crystal structure which shows (Fig. 6) that 1/2[100] is a perfect lattice repeat of the oxygen sublattice. It is then possible from the knowledge of the partial separation to evaluate the stacking fault energy. This calculation has been done using DISDI, which yields a stacking fault energy of the order of 110 mJ m^{-2}. The total energy of this dissociated configuration has been calculated and plotted in Fig. 5. Dissociation induces a significant energy reduction, which might explain that slip is activated in {021}, although Si–O bond breaking is required.

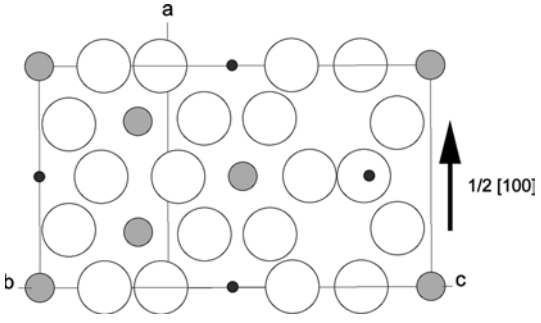

Fig. 6 Layer (4 Å thick) of wadsleyite parallel to (021). It is shown that 1/2[100] is approximately a repeat of the oxygen sublattice

1/2⟨111⟩ slip

As [100] slip, 1/2⟨111⟩ slip in {101} seems to play an important role in the plastic deformation of wadsleyite. 1/2⟨111⟩ dislocations have been observed in image mode and characterized by LACBED in every sample, whatever their deformation mode. 1/2⟨111⟩ {101} is one of the slip systems activated in shear deformation experiments which are thought to be easily activated at high temperature (1300 °C). This was expected, as 1/2⟨111⟩ is one of the shortest lattice repeats and as {101} is a close-packed plane of the anionic sublattice. This slip system has already been reported by Dupas et al. (1994). The energy of a 1/2⟨111⟩ dislocation line is plotted in Fig. 7 as a function of the line character. It is almost twice the energy of a [100] dislocation. However, 1/2⟨111⟩ dislocations have often been observed to be dissociated in two partials. Such an observation has already been reported in Dupas et al. (1994). Once again, the Burgers vector of the partials has not been unambiguously characterized; however, the two partials have a similar contrast, and they are in contrast with 400, 080, 004 and 303 diffraction vectors. This leads us to propose the simple dissociation reaction:

$$1/2[111] \rightarrow 1/4[111] + 1/4[111] \ .$$

The width of the faulted ribbon between the partials has been observed to range between 15 and 35 nm. This corresponds to a maximum stacking fault energy of 210 mJ m^{-2}. The line energy of the dissociated dislocation

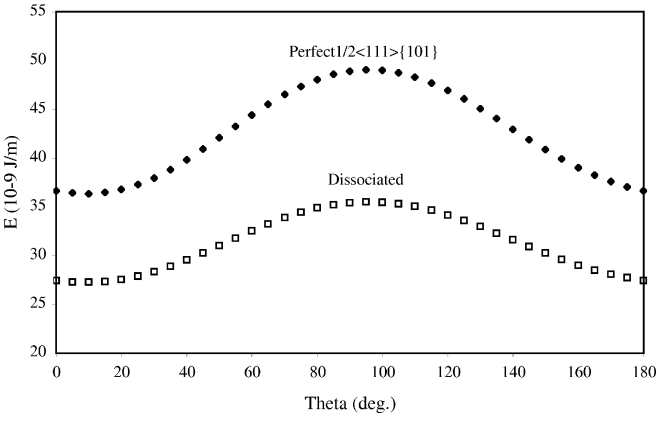

Fig. 7 Elastic energy per unit length of 1/2⟨111⟩ dislocations lying in {101} calculated with DISDI (*solid diamonds*). Theta represents the dislocation character (theta = 90° for the edge dislocation and theta = 0° or 180° for the screw dislocation). The *open squares* represent the elastic energy per unit length of 1/2⟨111⟩ dislocations dissociated in {101} into two 1/4⟨111⟩ partial dislocations separated by a stacking fault with an energy of 210 mJ m^{-2}

is plotted in Fig. 7, and is close to the energy values of [100] dislocations.

[010] slip

Except for one sample (H1433 see Part I), [010] dislocations have been observed in every sample deformed in compression. These dislocations are found to glide in (001) and {101}. The occurrence of dislocations with such a large Burgers vector (11.45 Å) is surprising, because it leads to a very high elastic energy (Fig. 8). We have analyzed the stability of [010] dislocations with respect to dislocations with smaller Burgers vectors. Figure 9 shows the possible decomposition of a [010] dislocation into two $1/2\langle 111\rangle$ dislocations in a {101} plane. The stability of a dislocation is usually given by the Frank criterion, which compares the relative energies of the original dislocation with that of the decomposition products. This can be done in more detail by calculating the line energies of the two configurations. Figure 10 presents the result of such a calculation. One can see that [010] dislocations are unstable. The energy difference is, however, minimum for the [010] screw orientation, which is the one for which the decomposition is geometrically possible. It should be noted that evidence of screw [010] dislocations exhibiting a double contrast compatible with this decomposition has been observed in several cases. In some other cases, the [010] dislocation lines are split into four lines with similar contrasts. These partial dislocations are in contrast with $g = 080$ and out of contrast with $g = 400$. We suggest that this dissociation might follow the simple scheme:

$$[010] \rightarrow 1/4[010] + 1/4[010] + 1/4[010] + 1/4[010] \ .$$

Indeed, it is shown in Fig. 11 that 1/4[010] is a repeat of the oxygen sublattice in (001). 1/4[010] shear introduces

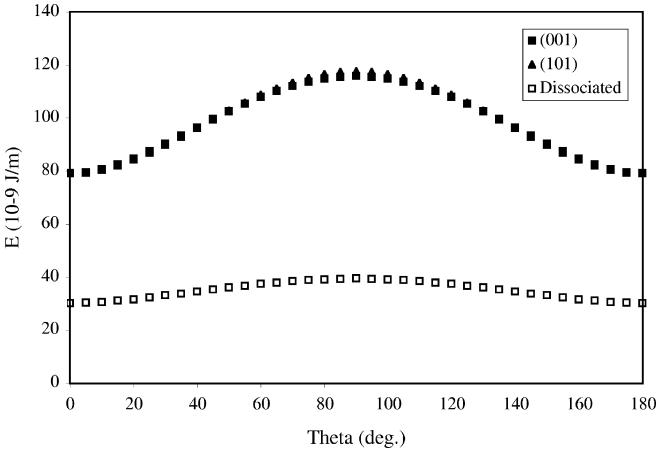

Fig. 8 Elastic energy per unit length of [010] dislocations lying in (101) and (001) calculated with DISDI (*solid symbols*). Theta represents the dislocation character (theta = 90° for the edge dislocation and theta = 0° or 180° for the screw dislocation). The *open squares* represent the elastic energy per unit length of a [010] dislocation dissociated in (001) into four 1/4[010] partial dislocations as calculated in Appendix 2

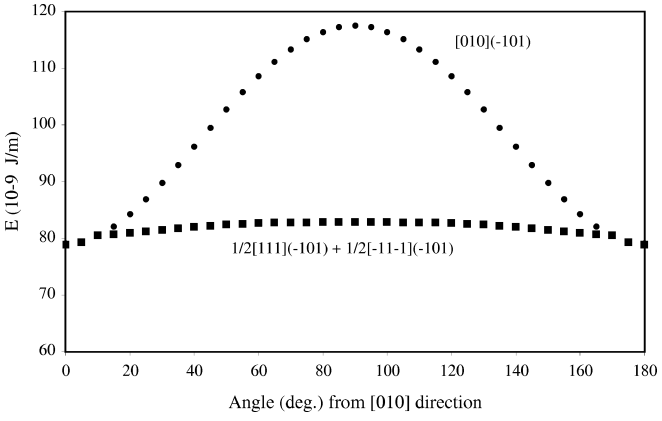

Fig. 10 Stability of [010] dislocations. Comparison of the elastic energy per unit length of a [010] dislocation lying in (-101) with the one of two $1/2\langle 111\rangle$ dislocations lying in the same plane (calculated with DISDI). Theta represents the angle between the line directions and [010]; this corresponds to the dislocation character for the [010] dislocation only

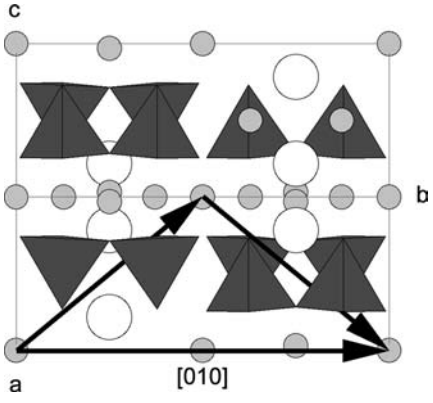

Fig. 9 Unit cell of wadsleyite viewed along the plane (101). Only the SiO_4 tetrahedra are represented. The decomposition of [010] in two $1/2\langle 111\rangle$ vectors is shown

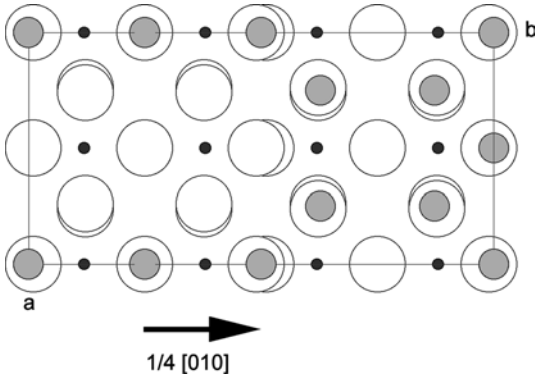

Fig. 11 Unit cell of wadsleyite viewed along [001]. No polyhedra are represented. It is shown that 1/4[010] is approximately a repeat of the oxygen sublattice

a cationic disorder only, with a stacking fault energy which is probably low. This might explain the relatively large partial dislocations separation observed. We have calculated the energy of a dislocation [010] dissociated into four partial dislocations 1/4[010] in the (001) plane. The details of the calculation are presented in Appendix 2. The total width of the dissociation is 200 nm as in Fig. 9 of Part I. This yields to stacking fault energies that are of the order of 40 to 60 mJ m^{-2}. It is shown in Fig. 8 that the energy reduction associated with this dissociation exceeds 50%. It must be remembered at this point that we have considered glide dissociation only. Some climb dissociation has also been observed that results from annealing and relaxation of the microstructure, but which is not discussed here.

⟨101⟩ slip

⟨101⟩ dislocations have only rarely been identified in image mode although their occurrence is demonstrated unambiguously by 13 LACBED characterizations. The magnitude of the ⟨101⟩ Burgers vector implies a high dislocation line energy, as shown in Fig. 12. However, energy calculations show that ⟨101⟩ dislocations are stable with respect to the Frank criterion (compared to 1/2⟨111⟩ dislocations, for instance). In several cases, however, we have observed partial dislocations with Burgers vectors compatible with 1/2⟨101⟩ (they have not been fully characterized by LACBED) gliding in (010). These partial dislocations might result from the dissociation reaction:

$$\langle 101\rangle \rightarrow 1/2\,\langle 101\rangle + 1/2\,\langle 101\rangle \ .$$

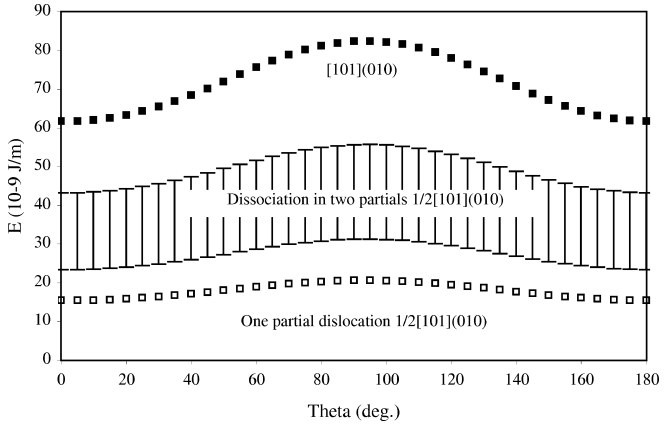

Fig. 12 Elastic energy per unit length of ⟨101⟩ dislocations lying in (010) calculated with DISDI. Theta represents the dislocation character (theta = 90° for the edge dislocation and theta = 0° or 180° for the screw dislocation). The *solid squares* represent the elastic energy per unit length of perfect dislocations. Dissociation into two 1/2⟨101⟩ partials is plotted for stacking fault energies in the range 0–200 mJ m^{-2}. The energy of a single 1/2⟨101⟩ partial dislocation is also represented (*open squares*), the stacking fault energy is not considered in this case

We tried to estimate the energy associated with this dissociated configuration. Such a calculation requires the input of the stacking fault energy. In the previous cases, these data were deduced from the equilibrium width of the dissociated dislocation. In the present case, the faulted ribbons are extended and do not exhibit any equilibrium width. This probably reflects a low stacking fault energy. Indeed, a 1/2⟨101⟩ (010) fault probably has the same structure as the faults observed in many wadsleyite samples (Madon and Poirier 1983; Price 1983; Dupas et al. 1994; Sharp et al. 1994; Mosenfelder et al. 2000), natural or not, and identified by Madon and Poirier as a thin (one or two atomic layer) layer with the ringwoodite structure. As a theoretical experiment, we have plotted in Fig. 12 the range of dislocation line energies of ⟨101⟩ dislocations dissociated into two 1/2⟨101⟩ partial dislocations separated by a stacking fault with an energy of between 0 and 200 mJ m^{-2}. The microstructures observed at the TEM can be alternatively interpreted as resulting from the direct nucleation of partial 1/2⟨101⟩ dislocation loops. The line energy associated with a single 1/2⟨101⟩ is also presented in Fig. 12. The values presented should be regarded as a lower limit, as the stacking fault energy (presumed to be small, but unknown) has not been taken into account.

[001] slip

The case of [001] slip is less straightforward. [001] dislocations have been detected only rarely and their occurrences have been interpreted as resulting from dislocation reactions. It seems thus that [001] slip is not activated. We have calculated the line energy associated with [001] slip in a number of planes containing the [001] direction (Fig. 13). As always, the elastic anisotropy appears to be weak, and the hypothesis made on the slip

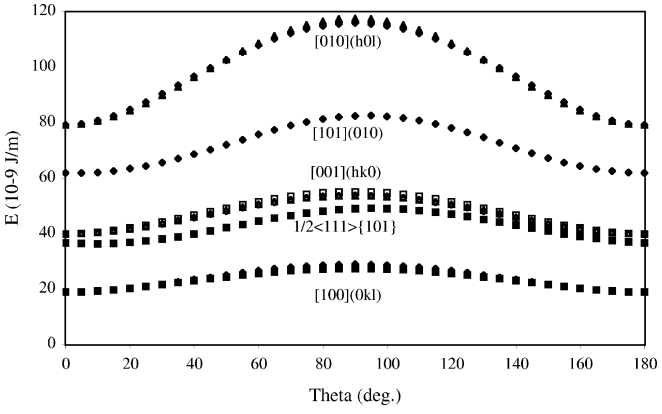

Fig. 13 Elastic energy per unit length of [001] dislocations lying in various (hk0) planes (*open symbols*) calculated with DISDI. Theta is the dislocation character (theta = 90° for the edge dislocation and theta = 0° or 180° for the screw dislocation) in any case. The elastic energies per unit length of the other slip systems (*perfect dislocations*) are plotted on the same graph for comparison

plane is not important. One can see in Fig. 13 that, from the energetic point of view, [001] slip is more favourable than ⟨101⟩ and [010] slip, and very close to 1/2⟨111⟩ slip! To overcome this apparent paradox, it should be remembered that much evidence for dislocation dissociations has been observed. The previous sections have shown that a significant reduction in the line energy often results from the dissociation. To illustrate this point, Fig. 14 compares the line energy of [001] dislocations with those of other dislocations but, contrary to Fig. 13, and as a theoretical experiment, we have systematically taken into account the dissociated configurations. In the case of ⟨101⟩ slip, we have even plotted the single 1/2⟨101⟩ partial. In this case, the energy associated with [001] dislocations appears significantly larger than that of other dislocations. A tentative conclusion of this analysis could be that, for some unknown reason, [001] dislocations have no favourable possibility of dissociation which prevents [001] slip from being activated.

Conclusion

The slip systems activated in wadsleyite during high-pressure deformation experiments are discussed based on crystal chemistry and anisotropic linear elasticity. It is shown that:

- wadsleyite is very isotropic from the elastic point of view;
- the slip planes are usually chosen among planes that do not need to break the strong Si–O bonds
- dissociation of dislocations significantly decreases the energy of dislocations; it is necessary to take dissociation into account to explain the relative ease of slip of the various slip systems.

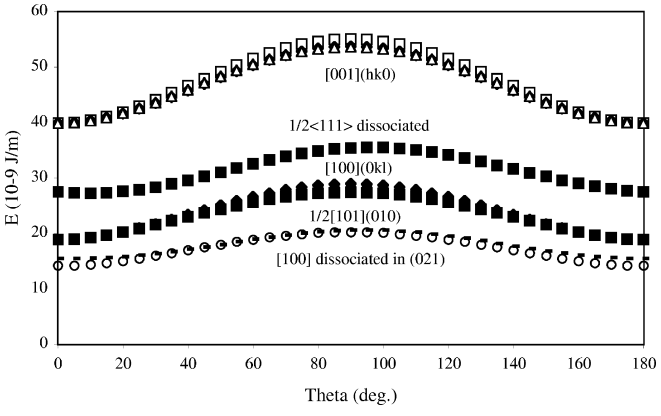

Fig. 14 Elastic energy per unit length of [001] dislocations lying in various (hk0) planes (*open symbols*) compared with the elastic energy per unit length of the other slip systems when dissociated dislocations are considered (calculated with DISDI). Theta is the dislocation character (theta = 90° for the edge dislocation and theta = 0° or 180° for the screw dislocation) in any case

We are aware that in this study a number of interpretations on the precise nature of the dissociation and core structure of dislocations are speculative, although based on a reasonable basis. These speculations were useful to point out the importance of dissociation on the plasticity of wadsleyite. It seems necessary, however, to carry out further detailed investigation on the precise core structure of the dislocations in wadsleyite to better understand and model the plastic behaviour of this mineral.

Acknowledgements High-pressure experiments were performed at the Bayerisches Geoinstitut under the EU IHP – Access to Research Infrastructures Programme (Contract no. HPRI-1999-CT-00004 to D.C. Rubie). Enlightening discussions with A. Coujou and J. Rabier are gratefully acknowledged.

Appendix 1: Calculation of the shear modulus $\mu_{[100](0kl)}$

The crystal is referred to a crystallographic basis (1, 2, 3) built on the unit cell. It is stressed (σ) along [100] in a plane (0kl) which makes an angle α with (001). A new reference basis is built on the following vectors: 1', the stress direction, is parallel to 1. 3′ is the normal of the shear plane. 2′ is chosen for (1′, 2′, 3′) to be right-handed (Fig. 15).

In (1′, 2′, 3′), the stress tensor has the simple form:

$$\bar{\bar{\sigma}}' = \begin{pmatrix} 0 & 0 & \sigma \\ 0 & 0 & 0 \\ \sigma & 0 & 0 \end{pmatrix}$$

It is possible to obtain the strain tensor by applying Hooke's law $\bar{\bar{\sigma}} = \bar{\bar{\bar{\bar{C}}}} \cdot \bar{\bar{\varepsilon}}$ However, the elastic constant tensor is given in (1, 2, 3) only. It is thus necessary to express the stress tensor in (1, 2, 3). The components in the new basis are given by: $\sigma_{ij} = \langle i|i'\rangle\langle j|j'\rangle\sigma_{i'j'}$ which yields:

$$\bar{\bar{\sigma}} = \begin{pmatrix} 0 & \sigma\sin\alpha & \sigma\cos\alpha \\ \sigma\sin\alpha & 0 & 0 \\ \sigma\cos\alpha & 0 & 0 \end{pmatrix},$$

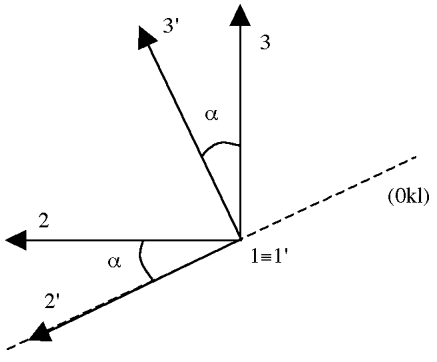

Fig. 15 Respective orientations of the reference basis (1, 2, 3) and (1′, 2′, 3′)

which in the matrix notation of Voigt is written as:

$$[\sigma] = \begin{bmatrix} 0 \\ 0 \\ 0 \\ 0 \\ \sigma\cos\alpha \\ \sigma\sin\alpha \end{bmatrix} .$$

It is then possible to obtain the strains from Hooke's law:

$$\begin{bmatrix} 0 \\ 0 \\ 0 \\ 0 \\ \sigma\cos\alpha \\ \sigma\sin\alpha \end{bmatrix} = \begin{bmatrix} C_{11} & C_{12} & C_{13} & 0 & 0 & 0 \\ C_{21} & C_{22} & C_{23} & 0 & 0 & 0 \\ C_{31} & C_{32} & C_{33} & 0 & 0 & 0 \\ 0 & 0 & 0 & C_{44} & 0 & 0 \\ 0 & 0 & 0 & 0 & C_{55} & 0 \\ 0 & 0 & 0 & 0 & 0 & C_{66} \end{bmatrix} \begin{bmatrix} \varepsilon_1 \\ \varepsilon_2 \\ \varepsilon_3 \\ \varepsilon_4 \\ \varepsilon_5 \\ \varepsilon_6 \end{bmatrix} ,$$

which yields:

$$\varepsilon_{12} = \frac{\sigma\sin\alpha}{2C_{66}} \quad \text{and} \quad \varepsilon_{13} = \frac{\sigma\cos\alpha}{2C_{55}} ,$$

and $\varepsilon_{1'3'} = \varepsilon_{12}\sin\alpha + \varepsilon_{13}\cos\alpha$.

Hence:

$$\mu_{[100](0kl)} = \frac{1}{\left(\frac{\sin^2\alpha}{C_{66}} + \frac{\cos^2\alpha}{C_{55}}\right)}$$

Appendix 2: Line energy of a [010] dislocation dissociated in four 1/4[010] partial dislocations

Let us consider the dissociation reaction proposed previously, (Fig. 16):

$$[010] \rightarrow 1/4[010] + 1/4[010] + 1/4[010] + 1/4[010]$$

The energy of the dissociated configuration is the sum of the self-energies of the partial dislocations plus their interaction elastic energies, plus the stacking fault energies:

$$E_T = \Sigma E_{self} + \Sigma E_{int} + \Sigma E_{fault} .$$

The interaction energy is written as:

$$\Sigma E_{int} = K_{12}\cdot \mathrm{Ln}\frac{d_1}{R} + K_{13}\cdot \mathrm{Ln}\frac{d_1+d_2}{R} + K_{14}\cdot \mathrm{Ln}\frac{d_1+d_2+d_3}{R} + K_{23}\cdot \mathrm{Ln}\frac{d_2}{R} + K_{24}\cdot \mathrm{Ln}\frac{d_2+d_3}{R} + K_{34}\cdot \mathrm{Ln}\frac{d_3}{R} .$$

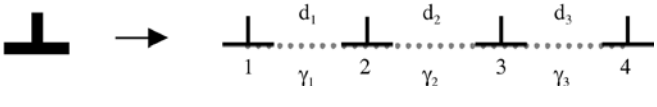

Fig. 16 Representation of [010] dislocations dissociation reaction

In the present case, the partial dislocations are parallel and supposed to be identical, so:

$$K_{12} = K_{13} = K_{14} = K_{23} = K_{24} = K_{34} = K_{int} .$$

K_{int} is a pair interaction coefficient which is a function of the orientation of the line. It can be calculated with DISDI for the interaction of two 1/4[010] partial dislocations lying in (001). The result of the calculation is shown in Fig. 17. The contribution of the stacking fault ribbons to the total energy is:

$$\Sigma E_{fault} = \gamma_1\cdot d_1 + \gamma_2\cdot d_2 + \gamma_3\cdot d_3 .$$

The equilibrium configuration is reached when the energy is minimized:

$$\frac{\partial E_T}{\partial d_1} = \frac{\partial E_T}{\partial d_2} = \frac{\partial E_T}{\partial d_3} = 0 ,$$

which yields the three following equations:

$$\frac{K_{int}}{d_1} + \frac{K_{int}}{d_1+d_2} + \frac{K_{int}}{d_1+d_2+d_3} + \gamma_1 = 0$$

$$\frac{K_{int}}{d_1+d_2} + \frac{K_{int}}{d_1+d_2+d_3} + \frac{K_{int}}{d_2} + \frac{K_{int}}{d_2+d_3} + \gamma_2 = 0$$

$$\frac{K_{int}}{d_1+d_2+d_3} + \frac{K_{int}}{d_2+d_3} + \frac{K_{int}}{d_3} + \gamma_3 = 0 .$$

The spacings d_i between the partial dislocations are measured on the micrographs, one obtains for the screw orientation:

$$d_1 = 90\,\mathrm{nm}, \quad d_2 = 65\,\mathrm{nm}, \quad d_3 = 45\,\mathrm{nm} ,$$

which yields to the stacking fault energy values:

$$\gamma_1 = 38\,\mathrm{mJ\ m^{-2}}, \quad \gamma_2 = 61\,\mathrm{mJ\ m^{-2}}, \quad \gamma_3 = 62\,\mathrm{mJ\ m^{-2}} .$$

It is then possible to calculate the total energy, which is plotted Fig. 8

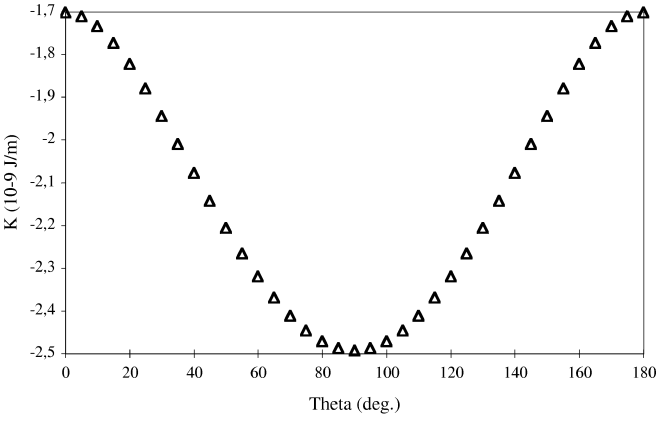

Fig. 17 Representation of the pair interaction coefficient between partial dislocations as a function of the orientation of the line (Theta is the angle between the line and the Burgers vector)

References

Dupas C, Doukhan N, Doukhan JC, Green II HW, Young TE (1994) Analytical electron microscopy of a synthetic peridotite experimentally deformed in the β olivine stability field. J Geophys Res 99: 15821–15832

Gwanmesia GD, Rigden S, Jackson I, Liebermann RC (1990) Pressure dependence of elastic wave velocity fo β-Mg_2SiO_4 and the composition of the Earth's mantle. Science 250: 794

Head AK, Humble P, Clareborough LM, Morton J, Forwood CT (1973) Defects in crystalline solids. North Holland Amsterdam

Li B, Gwanmesia GD, Liebermann RC (1996) Sound velocities of olivine and beta polymorphs of Mg_2SiO_4 at Earth's transition zone pressures. Geophys Res Lett 23: 2259–2262

Li B, Liebermann RC, Weidner DJ (1998) Elastic moduli of wadsleyite (β-Mg_2SiO_4) to 7 gigapascals and 837 kelvin. Science 281: 675–677

Li B, Liebermann RC (2000) Sound velocities of wadsleyite β-$(Mg_{0.88}Fe_{0.12})_2SiO_4$ to 10 GPa. Am Mineral 85: 292–295

Liebermann RC, Li B (1998) Elasticity of deep Earth materials at high pressures and temperatures. Ultrahigh-pressure Mineralogy: Physics and Chemistry of the Earth Interior. R.J. Hemley, Mineralogical Society of America 37: 459–492

Liebermann RC (2000) Elasticity of mantle minerals (experimental studies). In: Earth's deep interior: mineral physics and tomography: from the atomic to the global scale. American Geophysical Union, Washington, DC, pp 181–199

Madon M, Poirier JP (1983) "Transmission electron microscope observation of α, β and γ (Mg, Fe)$_2$ SiO_4 in shocked meteorites: planar defects and polymorphic transitions." Phys Earth Planet Int 33: 31–44

Mosenfelder JL, Connolly JAD, Rubie DC, Liu M (2000) Strength of (Mg, Fe)$_2SiO_4$ wadsleyite determined by relaxation of transformation stress. *Phys Earth Planet Int* 120: 63–78

Price GD (1983) "The nature and significance of stacking faults in wadsleyite, natural β-(Mg, Fe)$_2SiO_4$ from the Peace River meteorite." Phys Earth Planet Int 33: 137–147

Sawamoto H, Weidner DJ, Sasaki S, Kumazawa M (1984) Single-crystal elastic properties of the modified β-phase of magnesium orthosilicate. Science 224: 749–751

Sharp TG, Bussod GY, Katsura T (1994) Microstructures in β-$Mg_{1.8}Fe_{0.2}SiO_4$ experimentally deformed at transition-zone conditions. Phys Earth Planet Int 86: 69–83

Sinogeikin SV, Katsura T, Bass JD (1998) Sound velocities and elastic properties of Fe-bearing wadsleyite and ringwoodite. J Geophys Res (B) 103: 819–825

Sixtrude L (2000) Elasticity of mantle phases at high pressure and temperature. Earth's deep interior: mineral physics and tomography: from the atomic to the global scale. Karato SI, Forte AM, Liebermann RC, Masters G, Sixtrude L (eds) American Geophysical Union 117: 201–213

Stroh AN (1958) Dislocations and cracks in anisotropic elasticity. Phil Mag 3: 625–646

Zha CS, Duffy TS et al. (1998) Single crystal elasticity of the α and β polymorphs of Mg_2SiO_4 at high pressure. Properties of Earth and planetary materials at high pressure and temperature. Manghnani MH, Yagi T (eds) Washington, DC, American Geophysical Union 101: 9–16